Al_2Ni_3 PRECIPITATION INDUCED BY ELECTRON BEAM IRRADIATION

D.L.Liu[1] *and H.Hashimoto*[2]

1) Department of Materials Physics, University of Science and Technology Beijing, Beijing 100083, China
2) Department of Mechanical Engineering, Okayama University of Science, Japan

An as-quenched Cu-11.2%(wt)%Al-2.9(wt)%Ni alloy specimen, which consists of ordered N9R and 2H structure martensites, was examined by a 400 kV TEM. Large numbers of dispersive precipitates in the specimen are induced by the electron beam irradiation. These fine particles are identified as Al_2Ni_3 phase by electron diffraction. The stereoscopic measurement of the dark field TEM images combined with HREM study showed that this irradiation induced precipitation is not only a surface reaction. Al_2Ni_3 particles precipitate preferentially at crystalline defects and interfaces of the martensitic matrix. When duration of the electron beam irradiation lengthens, growth and coarsening of the precipitates are also observed.

KEY WORDS Cu-Al-Ni alloy, electron microscopy, irradiation effects, precipitation of Al_2Ni_3, martensitic structure

1 Introduction

As already known, during a transmission electron microscope examination, the incident electrons interact strongly with both atomic nuclei and atomic electrons of the solid specimen. This interaction can lead to permanent atom displacement and the attendant vacancy. In other words, Frenkel defects are created in the specimen by the beam irradiation. In presence of a high concentration of Frenkel pairs (for example the concentration $\sim 10^{-4}$) the interaction between defects will induce grosser atomic rearrangements. Such structural change in irradiated specimens includes faults, dislocation loops, disordering, ordering, decomposition, precipitation and compositionally-drived phase transformations [1]. Examples of the precipitation induced by electron beam irradiation in metallic alloys under TEM observations have been reported such as precipitation in Pt-C, Fe-Cu, Al-Si, Al-Ge, Fe-Ni, *etc.* [2].

On the other hand, efforts have been devoted to study the mechanism of phase transformations by electron microscopes. In order to clarify the mechanisms of the transformation processes, various induced phenomena by high energy electron beam have to be considered. For example, transport properties in an irradiated specimen area are altered because Frenkel pairs concentration changing. Moreover, the energy stored in atomic displacements and the entropy considerations can appreciably alter the thermodynamics of the phase equilibrium. Thus, the effects of beam irradiation on the primary phase transformation have to be investigated in detail. The experimental results from TEM observations have to be carfully judged whether these results really represent the processes in a bulk specimen. In the present work, a near eutectoid copper-aluminum system with small amount of Ni addition was prepared,

heat-treated and investigated mainly by electron microscopy. Some preliminary results about the effect of 400 keV electron beam irradiation on the precipitation of Al_2Ni_3 phase in a Cu-11.2Al-2.9Ni (wt)% alloy will be presented and discussed.

2 Experiment

The experimental alloy sample was prepared in laboratory by melting pure copper and aluminum (99.9%) in argon atmosphere. Chemical analysis showed that composition of the alloy samples is Cu-11.2(wt)%Al-2.9(wt)%Ni. After homogenization at 1173 K, the ingots with diameter 20 mm were peeled off their skin by machinery, then cut into small pieces about 6 mm in diameter and 0.5 mm thick. The samples were reheated up to 1173 K for 1 h in argon atmosphere followed by quenching into iced brine. Afterwards, these discs were thinned by manually grinding before the final procedure of the specimen preparation by argon ion beam milling at 4.5 kV and current 0.8 mA. TEM observations were carried out on a JEOL JEM 4000EX microscope operated at 400 kV with electron flux about 6×10^{18} electrons / $(cm^2 \cdot s)$.

3 Results and Discussion

### 3.1 The martensite structure in the sample

TEM examinations combined with electron diffraction study showed that the fresh specimen of this alloy, which was quenched from 1173 K and thinned by argon ion beams (at 4.5 kV and 0.8 mA current for typical period of 12 h), consists of two kinds of martensitic structures. One of the martensites possesses M2H structure, it consists of many microtwins. The other martensite is consistent with a ordered N9R structure and contains large number of stacking faults. X-ray diffraction results from a bulk specimen also confirmed that there exist the ordered N9R and 2H martensite structures in the quenched specimens. The detailed description of these martensite structures in the alloy is presented elsewhere [3] . It is already known from the previous work that the 2H martensite in this alloy is characterized by three microtwin variants with twinning planes {121}, {210} and {101}. Fig.1a shows a TEM micrograph of the 2H type martensite. The corresponding electron diffraction pattern shown in Fig.1c was taken from a fresh specimen area, which shows only diffraction spots of the martensite along zone axis [124] superposed on its twin spots pattern. A dark field TEM image of the 2H martensite formed by its reflections $\overline{4}2\overline{2}$ (index of the reflections is in Fig.1c) is shown in Fig.1b. TEM bright field image of a martensite plate with N9R structure and its electron diffraction pattern [110] are shown in Fig.2a and 2b respectively. The fringe contrast in Fig.2a and the diffuse string and extra weak spots between every two main diffraction spots of the 9R structure in Fig.2b are resulted from the stacking faults in the martensite plate. It is obvious that each diffraction pattern of both martensites are resulted from a single crystal of either martensite. There are few or no small precipitates in the specimen except martensites.

3.2 Effect of electron irradiation on precipitation

In general, irradiation of solids by high energy electrons can result in a number of processes including the replacement and displacement of atoms. There is a consequent increase in the concentration of vacancies and interstitials. These excess point defects induced by the electron beam could enhance atomic diffusion in the specimen. Therefore, precipitation or decomposition during the irradiation may occur.
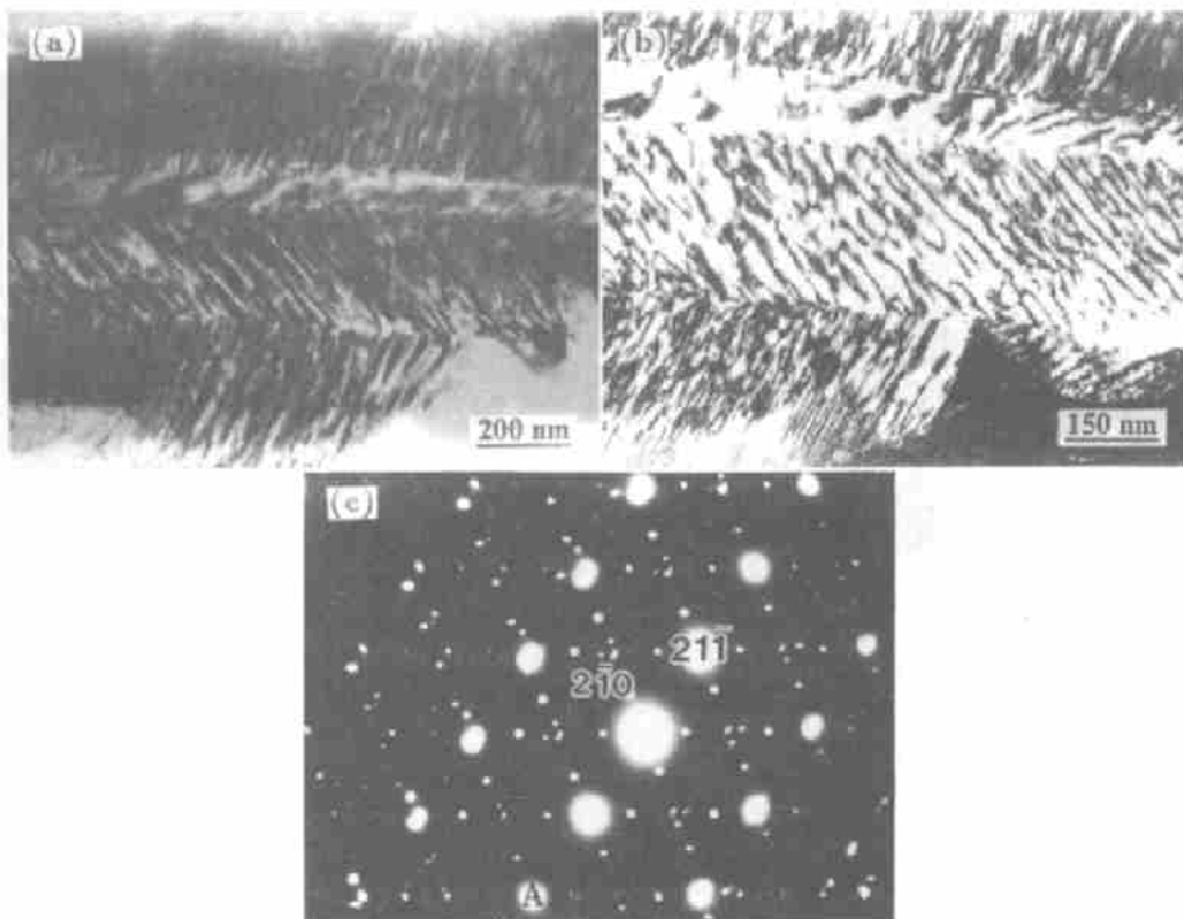
Fig.1 (a) TEM micrograph of the M2H martensite in as-quenched sample.   (b) Dark field image formed by the reflections within the circle A in Fig.1c.   (c) Electron diffraction pattern (124)* taken from a fresh specimen area of the martensite and its twins.
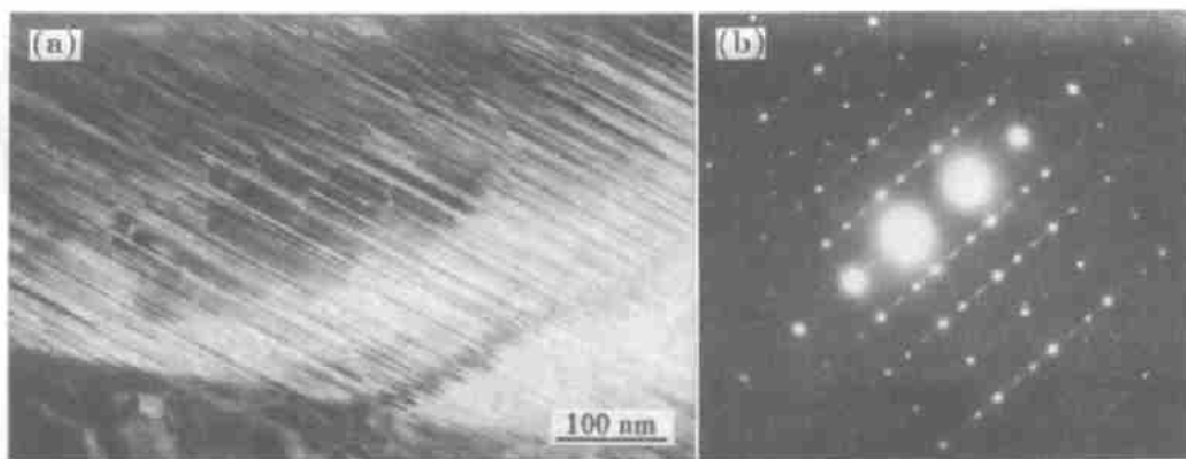

Fig.2 (a) TEM bright field image of a 9R martensitic plate in the specimen.   (b) Electron diffraction pattern [110] of the 9R martensite.

In order to examine the effects of electron beam irradiation on structure of the as-quenched Cu-Al-Ni specimen, a selected specimen area was set in the TEM under an incident beam with 400 keV energy and flux about 6×10^{18} electrons / (cm^2 · s) continuously for hours. When the specimen area is irradiated for certain period, large number of small particles form in the irradiated area. This is clearly indicated by electron diffraction patterns. When the specimen area is irradiated for 30 min by the electron beam, a weak diffraction ring appears, which superposed on the spot diffraction pattern. After more than one hour irradiation several diffraction rings can be seen. The diffraction patterns taken from an area irradiated for 80 min and for 5.5 h are shown in Fig.3a and Fig.3b respectively. Large number of small particles distributed in the martensitic matrix are clearly observed in dark field TEM images such as shown in Fig.4. This image was formed by diffraction beams within a circle
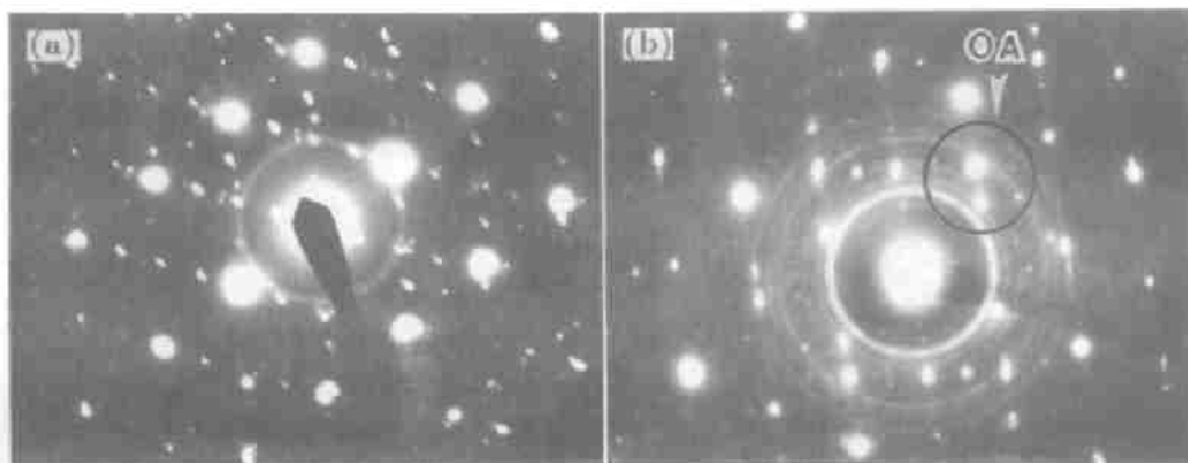
Fig.3 (a) Diffraction pattern taken from the same area as the pattern in Fig.1b but irradiated by electron beam for 80 min.   (b) Diffraction pattern from the specimen area irradiated for 5.5 h.
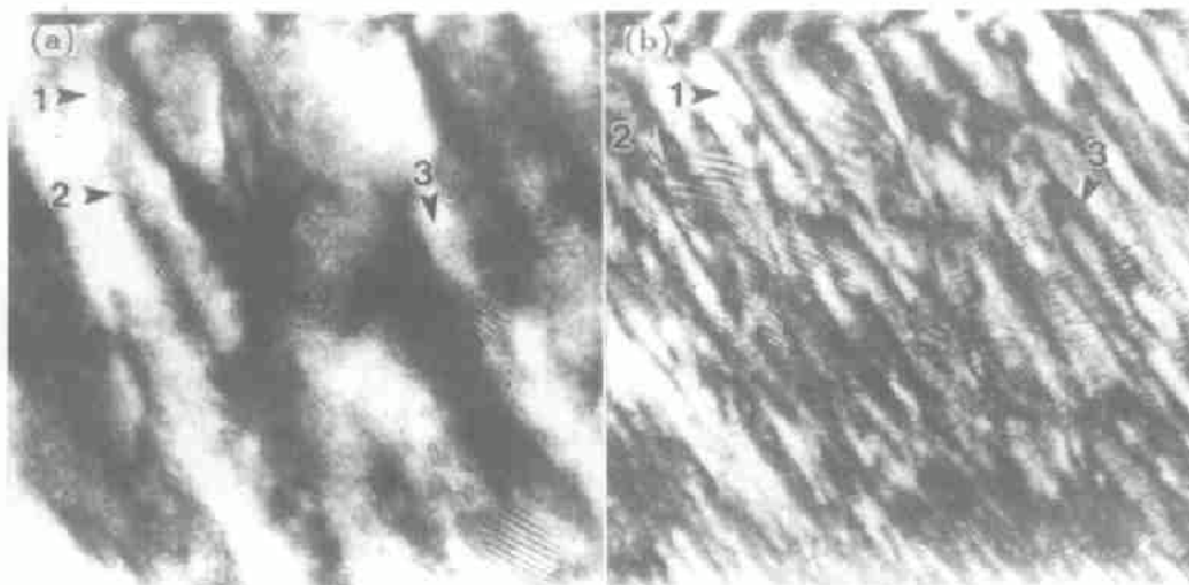

Fig.4 (a) TEM dark feild (DF) image of a specimen area irradiated by 400 keV electron beam for 0.5 h.
(b) DF image of the same area as in Fig.4a but irradiated for 5.5 h formed by diffraction beams within the circle OA shown in Fig.3b.

OA shown in Fig.3b. The crystalline interplanar spacings determined from the ring diffraction patterns such as Fig.3b are listed in Table 1 with those values of Al$_2$Ni$_3$ phase from

**Table 1** Interplanar spacings of the precipitated phase measured by electron diffraction, d_{exp}, and of Al$_2$Ni$_3$ phase, $d_{Al_2Ni_3}$.

No.	1	2	3	4	5	6	7	8	9	10
d_{exp}, nm	0.324	0.255	0.204	0.182	0.172	0.160	0.135	0.129	0.120	0.111
$d_{Al_2Ni_3}$, nm	0.324	0.267	0.206	0.189	0.163	0.162	0.139	0.133	0.123	0.119
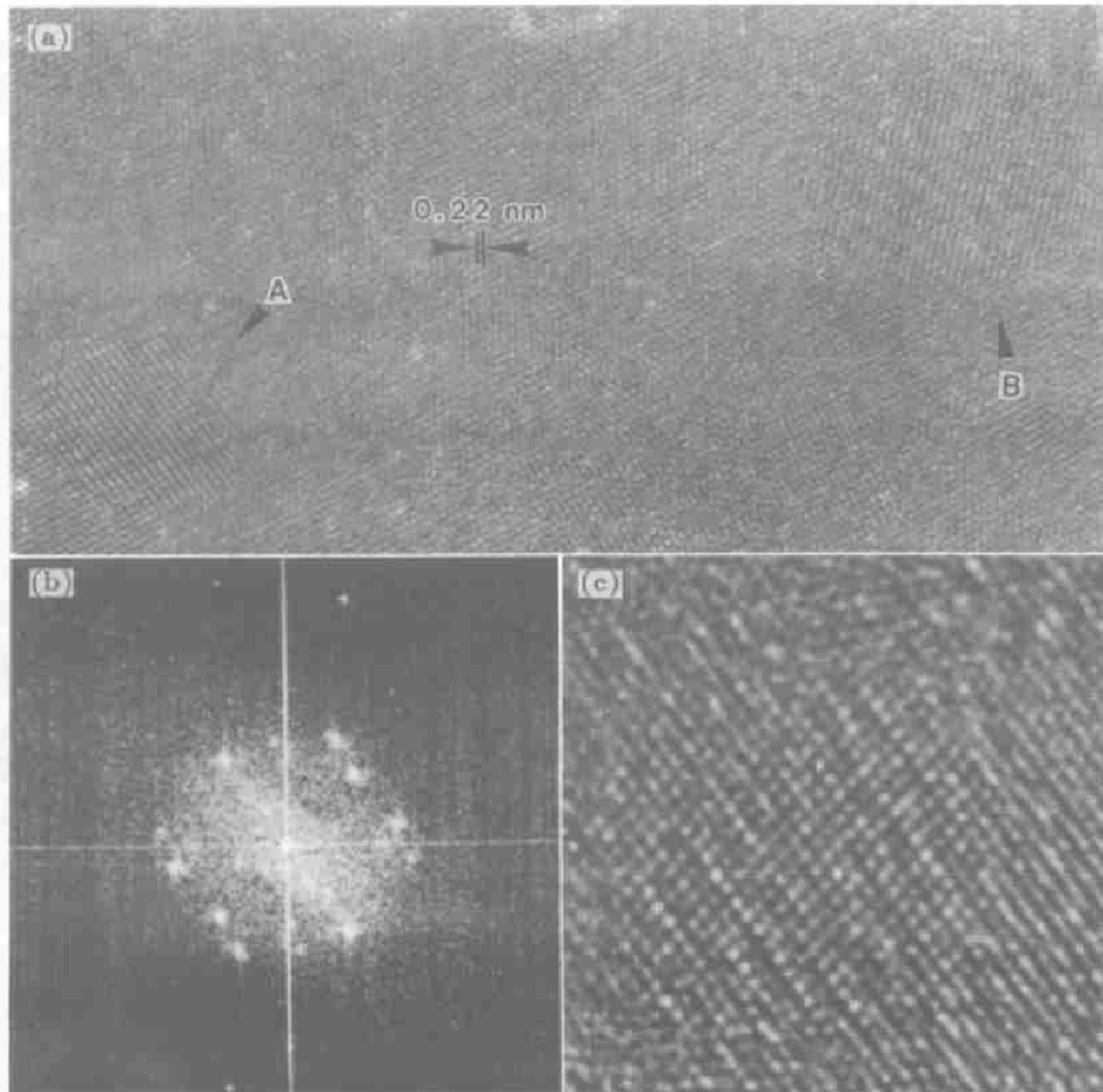
Fig.5 (a) HREM image showing precipitates marked with A and B, which are overlapped on 2H martensite. (b) A Fourier transform pattern of the precipitate A in Fig.5a.   (c) Reconstructed image of the precipitate A in Fig.5a.

reference [4] , which is a tetragonal structure with lattice parameters $a=b=0.267$ nm. $c=0.324$ nm and $c/a=1.2159$. It is obvious by comparison of these d-spacings that the precipitates are consistent with Al_2Ni_3 phase within reasonable error. These small particles are difficults to visualize on a TEM brigh field image because they are too small to create sufficient contrast in the image. But in a dark field image these fine particles can be recognized by their moire fringes owing to overlapping on the martensite matrix. They are quadrangular or sphere in shape. Their size is ranged from several nanometers to about 20 nm for a specimen area irradiated for 30 min by estimating of 15 particles on TEM picture. HREM image in Fig.5a shows precipitates with mark A and B overlapped on the 2H martensitic matrix. Fourier transform pattern of the particle A and reconstructed image are given in Fig.5b and 5c respectively. These particles are smaller than 10 nm in dimension and have coherent interface with the martensitic matrix. HREM image of Fig.6a shows two particles marked with A and B formed in the 9R martensitic matrix. The F.T.pattern and reconstructed image are given in Fig.6b and 6c respectively.
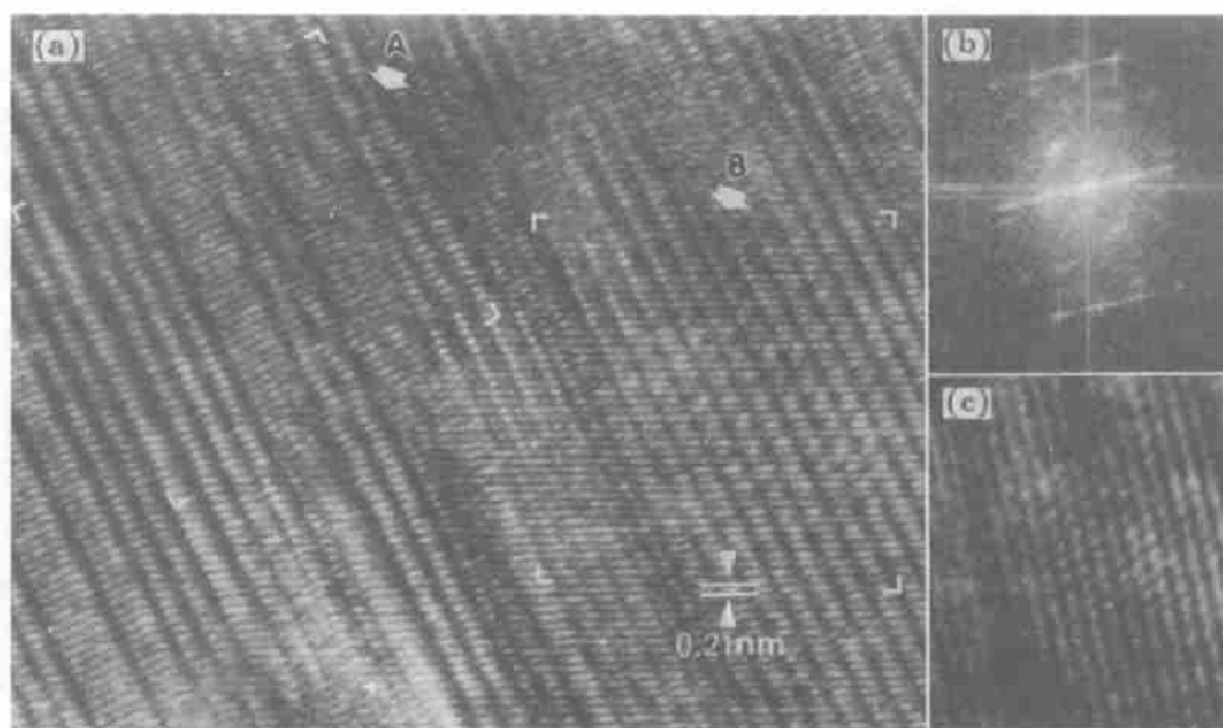

Fig.6 (a) Precipitates marked with A and B in a 9R martensitic matrix.   (b) F.T.pattern of the particle B in Fig.6a.   (c) Reconstructed image of the particle B by F.T.pattern in Fig.6b.

3.3 *Nucleation growth and coarsening of the Al_2Ni_3 phase*

In order to examine whether these Al_2Ni_3 precipitates only nucleate on the specimen surfaces or also in the interior of the specimen. stereoscopic observation technique was performed [5]. Dark field TEM images (DFI) were used for the stereoscopic measurement because these small precipitates can be much clearly visualized in the dark field image. The stereopair of DFI micrographs were taken from the same specimen area but tilted 10 degree around the X axes from one to the other. These stereopair pictures are shown in Fig.7a and Fig.7b respectively. Thirty three particles in Fig.7 were measured by using a stereometer. The

results showed that the Al_2Ni_3 precipitates distribute at different depths of the specimen. It is not only a surface reaction. Actually, the martensitic matrix provided large number of preferential sites for nucleation of the precipitates such as microtwin boundaries, martensitic interfaces, crystalline defects, *etc.*. An HREM image in Fig.8 shows that Al_2Ni_3 particles formed preferentially at one of those boundaries, though these microtwin boundaries themselves are unstable under the electron beam bombarding.
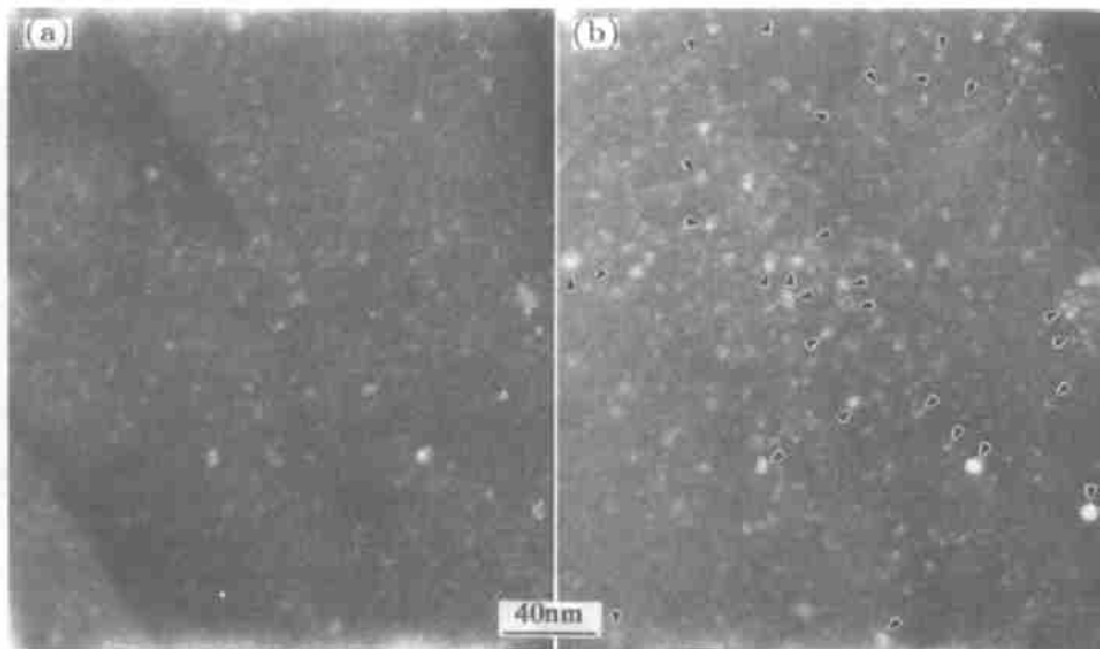
Fig.7 Stereo parir of dark field TEM images. The bright spots are Al_2Ni_3 particles in martensite matrix.

(a) tilt axis $X=0°$, $Y=0°$.   (b) $X= 10°$, $Y=0°$.

In an attempt to understand the kinetic process of the precipitation, a systematic study in the present work was carried out. It showed that when a specimen area is irradiated by electron beam for about 0.5 h only one diffraction ring could be recognized in the diffraction pattern. After one hour irradiation several diffraction rings due to Al_2Ni_3 precipitates have appeared. While the duration of electron irradiation lengthens, the intensity of the diffraction rings increases. This is resulted mainly from the growth and further nucleation of the precipitates. Furthermore, coarsening of the precipitates during the irradiation is also observed. As already discussed in above context, Fig.4a shows a dark field image of the specimen area irradiated for 0.5 h, whereas an image of exactly the same area but irradiated for 5.5 h is shown in Fig.4b. Some small particles pointed by number 1,2,3, *etc.* are clearly shown in Fig.4a. The same locations are pointed by the same numbers in Fig.4b. it can be seen by comparison of the two pictures that many precipitates already grown and some of them are connected to each other in the specimen area irradiated for 5.5 h. At the same time some of the small particles disappeared such as No.1 particle in Fig.4a, it is not showing in Fig.4b. Thus, the precipitation of Al_2Ni_3 phase induced by electron beam irradiation may also follow the three stages of a normal precipitation process: nucleation, growth and coarsening.
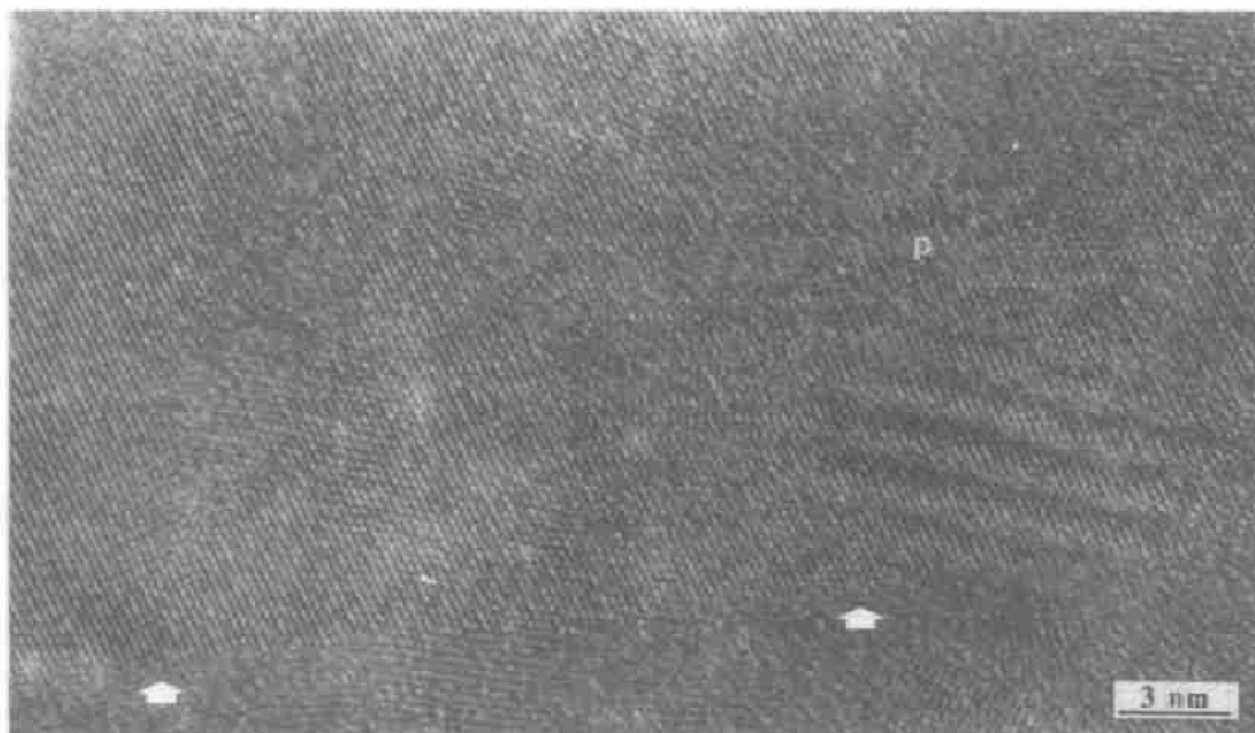
Fig.8   Precipitates formed preferentially at twin boundaries of the martensite

4   Summary

Irradiation by high energy electron beam may induce various structural changes in metal and alloy specimens during TEM examinations. When an as-quenched Cu–11.2(wt)%Al –2.9(wt)%Ni alloy specimen, which possesses N9R and 2H martensitic structures, is irradiated by 400 keV electron beam Al_2Ni_3 precipitation takes place. Stereoscopy study of the TEM dark field micrographs showed that this precipitation is not only a surface reaction. Fine dispersive Al_2Ni_3 particles precipitate preferentially at crystalline defects and interfaces of the martensites such as microtwin boundaries, stacking faults *etc.*, though the interfaces of the martensites are not stable under the beam irradiation. While duration of the electron beam irradiation lengthens, growth and coarsening of the Al_2Ni_3 precipitates is also observed in the specimen. The present study on the process of this precipitation confirmed that equilibrium phase diagrams can no longer be expected to apply under irradiation conditions [6-8]. Effects of high energy beam irradiation on the primary phase transformations in alloys have to be carefully considered in order to understand their real mechanisms.

REFFERENCES

1 L.W.Hobbs, *Introduction to Analytical Electron Microscopy*, eds. J.J.Hren, J.I.Goldstein and D.J.Joy (Plenum Press, New York, 1979) p.437.

2 K.H.Westmacott and U.Dahmen, *In situ Experiments with High Voltage Electron Microscopes*, ed. H.Fujita, (1985) p.137.

3 D.Liu, H.Hashimoto and T.Ko, *J.Mater.Sci.* (1996 in press).

4 V.L.Himes, M.J.Carr, R.Anderson *et al*, *Elemental and Interplanar Spacing Index for Phase Identification by Electron or X-ray Diffraction.* (1989)72.

5 M.Kiritani, *Electron Microsc.* **16**(2)(1981) 71 (in Japanese).

6 K.C.Russell, *Radiation Effects in Breeder Reactor Structural Materials*, eds. M.L.Bleiberg and J.W.Bennett (AIME, New York, 1977) p.821

7 L.E.Tanner, *Competing Interactions and Microstructures: Statics and Dynamics*, Proc. of the CMS Workshop, Los Alamos, New Mexico, May 5-8, 1987, eds. R.Lesar, A. Bishop and R.Heffner (Springer-Verlag, 1988).

8 K.Urban, S.Banerjee and J.Mayer, *Mater. Sci. Forum* **3** (1985) 335.

电子束辐照诱导 Al$_2$Ni$_3$ 相的析出

柳得櫓

(北京科技大学材料物理系、北京 100083)

H.Hashimoto

(Department of Mechanical Engineering, Okayama University of Science, Japan)

摘 要 用 400 kV 透射电镜观察由 N9R 及 2H 马氏体组成的淬火 Cu-11.2Al-2.9Ni 合金样品时, 发现大量弥散相因电子束辐照而析出. 电子衍射分析证实析出相为 Al$_2$Ni$_3$. 暗场像体视测量与高分辨显微术研究表明, 辐照诱导析出不仅是表面反应. Al$_2$Ni$_3$ 粒子择优在晶体缺陷及马氏体界面处析出. 延长辐照时间, 析出相长大并粗化.

关键词 Cu-Al-Ni 合金, 电子显微术, 辐照缺陷, Al$_2$Ni$_3$ 析出相, 马氏体结构